Soft Information Aided ML Joint Frame Synchronization and Channel Estimation for Downlink MC-CDMA in the Presence of Narrowband Interference

Mohamed Marey, Mamoun Guenach, Frederik Simoens, and Heidi Steendam
DIGCOM research group, TELIN Dept., Ghent University
Sint-Pietersnieuwstraat 41, 9000 Gent, BELGIUM
E-mail: {mohamed, guenach, fsimoens, hs}@telin.ugent.be

***Abstract*— Spectrum-overlay scenarios for wideband multi-carrier (MC) systems bring new technical challenges that must be considered during the system design. In such a scenario, the receiver has to perform actions, such as channel estimation and synchronization, in the presence of possibly strong in-band interference. In this paper, we modify the iterative maximum likelihood joint frame synchronization and channel estimation algorithm for downlink MC-CDMA presented in [1] to have better performance in the presence of narrowband interference. The performance of the modified algorithm is verified through computer simulations and compared with the original one.**

I. Introduction

Recently, multi-carrier (MC) systems have attracted an increasing interest due to their use in digital audio and video broadcasting services and to the possible adoption in Fourth-Generation (4G) mobile communication standards [2], [3]. One of the main advantages they offer is robustness against frequency selectivity encountered in high-rate wireless channels.

As the bandwidth resources are scarce, sometimes the MC system has to coexist with narrowband (NB) legacy systems that use the same bandwidth. The presence of these narrowband interference (NBI) hampers the proper action of the MC system. In [4]–[6], we have investigated the influence of the NBI on different data-aided synchronization algorithms for timing and frequency synchronization. In this paper, we extend our previous research by investigating the impact of digital modulated NBI on the iterative algorithm for joint channel impulse response estimation and frame synchronization in MC-CDMA proposed in [1]. Moreover, we modify the algorithm to have better performance in the presence of NBI.

The rest of the paper is organized as follows. In section II, a MC-CDMA system model and a narrow-band interference model are described. The derivation of the modified algorithm in the presence in NBI is illustrated in section III. Simulation results are shown in section IV. Finally, the conclusions are given in section V.

II. System Description

A. MC-CDMA System Model

In this section, we summarize the MC-CDMA system model proposed in [1]. The block diagram of a downlink MC-CDMA transmitter with M active users is shown in figure 1. Frame based transmission is assumed, where for every user each frame consists of X_c coded bits. The X_c coded bits are mapped on X_d symbols belonging to a 2^q point-constellation, $X_d = X_c/q$. The resulting X_d symbols are broken into B_s blocks of length Q, where $Q = X_d/B_s$. Further, the blocks of length Q are spread, S/P converted, interleaved in the frequency domain, converted to the time domain using an N-dimensional inverse Fourier transform (IFFT), and finally the cyclic prefix of length ν samples is inserted. We can write the n-th time-domain sample ($n = -\nu, \ldots, N-1$) of the j-th MC block of the k-th user as

$$s_{j,n}^{(k)} = \sqrt{\frac{E_s}{N+\nu}} \sum_{q=0}^{Q-1} \sum_{s=0}^{N_s-1} d_{j,q}^{(k)} c_s^{(k)} e^{j2\pi m_{q,s}^{(k)} n/N} \quad (1)$$

where $d_{j,q}^{(k)}$ is the q-th modulated data symbol at j-th MC-CDMA block for k-th user, $c_s^{(k)}$is the s-th chip of the N_s-dimensional spreading code of the k-th user, E_s denotes the energy per symbol, and $m_{q,s}^{(k)}$ is the index of the modulated subcarrier. We further define the MC block duration T and the sampling duration $T_s = T/N_T$, where $N_T = N + \nu$. The signals of the M different users are added, shaped with a normalized transmit filter and transmitted over the channel to the mobile stations. Finally, each data frame is preceded by B_p pilot MC blocks, to be able to estimate the channel taps $\mathbf{h}$ and the integer propagation delay Δ. A part of the subcarriers of the pilot MC blocks contains training symbols while the remainder of the carriers is taken up with administrative data.

B. Narrowband Interference Model

We assume the NBI consists of N_I digital modulated signals, as e.g. occurs in the (B-VHF) system [7]. Following the interference model from [5], [8], the interfering signal $x_I(t)$ can be written as

$$x_I(t) = \sum_{l=1}^{N_I} \sum_{i=-\infty}^{\infty} z_{h,l} p_l(t - iT_l - \tau_l)\, e^{j2\pi(f_0+f_{c,l})t} \quad (2)$$

where $f_{c,l}$ is the carrier frequency deviation from the MC central carrier frequency f_0 for the lth interferer, $p_l(t)$ is the time domain response of the transmit filter of the lth interferer, $z_{h,l}$ is the hth data symbol of the lth interferer, τ_l is its delay, and $1/T_l$ its sample rate. The total NBI signal at the output of the matched filter of the MC receiver is given as

$$r_I(t) = \sum_{l=1}^{N_I} \sum_{i=-\infty}^{\infty} z_{i,l}\, e^{j2\pi f_{c,l} i T_l}\, g_l(t - iT_l) \quad (3)$$

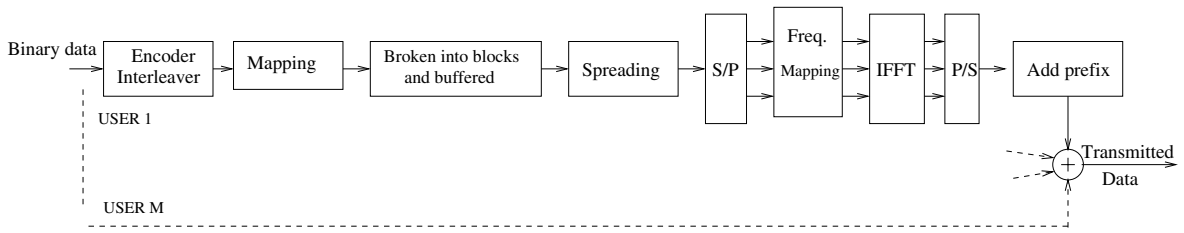

Fig. 1. Downlink MC-CDMA transmitter

where $g_l(t)$ is the convolution of $p_0(-t)$ and $p_l(t-\tau_l)\exp(j2\pi f_{c,l}t)$ and $p_0(t)$ is the time domain response of the MC-CDMA receiver filter. It is assumed that the interfering symbols are uncorrelated with each other, i.e. $E[z_{h,l}z^*_{h',l'}] = E'_l\delta_{ll'}\delta_{hh'}$, where E'_l is the energy per symbol of the lth interferer. Further, the interfering data symbols are statistically independent of the MC data symbols. The signal to interference ratio (SIR) at the input of the receiver is defined as [4]–[6]

$$SIR = \frac{2\sigma_s^2/T_0}{\sum_{l=1}^{N_I}\frac{E'_l}{T_l}} \tag{4}$$

where σ_s^2 is the variance of the MC transmitted sample per real dimension.

III. Soft Information Aided Joint ML Channel Estimation and Frame Synchronization Algorithm in the Presence of NBI

In [1], the delay Δ and the channel taps $\mathbf{h}$are estimated in an AWGN environment. In this section, we modify the estimation algorithm to estimate Δ and $\mathbf{h}$ in the presence of NBI. The conceptual block diagram of the receiver is shown in fig. 2. The receiver of user k' employs the ML algorithm to obtain initial estimates (e.g., by exploiting the B_p pilot MC symbols) $\left(\hat{\Delta},\hat{\mathbf{h}}\right)$ for the timing offset Δ and the channel taps $\mathbf{h}$ (iteration 0). Then, the a posteriori expectations of the transmitted symbols are computed. Although the a posteriori expectations of the symbols serve for decoding and data detection, they can also be used to iteratively improve the timing synchronization and channel estimation. As shown in [1], the received sequence $\mathbf{r} = [r(-\nu T_s),\ldots,r((B_s+B_p)T+(\Delta_{max}+L-\nu-2)T_s)]^T$ of $N_T(B_s+B_p)+\Delta_{max}+L-1$ time-domain samples is sufficient to synchronize, to estimate channel impulse response, and to detect the data, where Δ_{max} denotes to the maximum integer part of the propagation delay. This sequence contains the contributions of the B_p pilot blocks and B_s data blocks. We can write

$$\mathbf{r} = \mathbf{S}_\Delta\mathbf{h} + \mathbf{w} + \mathbf{Int} \tag{5}$$

where $\mathbf{h} = [h_0, h_1, ..., h_{L-1}]^T$ is the vector of the L channel taps, the vector $\mathbf{w}$ consists of the thermal noise, the Multiple Access Interference (MAI) can be modeled as a zero-mean complex Gaussian random variable with variance σ^2 per real dimension and the vector $\mathbf{Int}$ corresponds to the narrowband interference signal. Further, $\mathbf{S}_\Delta$ is a $(N_T(B_p+B_s)+\Delta_{max}+L-1)\times L$ matrix defined as

$$\mathbf{S}_\Delta = \begin{bmatrix} \mathbf{0}_{\Delta\times L} \\ \mathbf{S} \\ \mathbf{0}_{(\Delta_{max}-\Delta+L-1)\times L} \end{bmatrix}. \tag{6}$$

where $\mathbf{0}_{X\times Y}$ is the $X\times Y$ all zero matrix and $\mathbf{S}$ is a $(N_T(B_s+B_p)+L-1)\times L$ Toeplitz matrix consisting of two Toeplitz matrices: $\mathbf{S} = \mathbf{S}_P + \mathbf{S}_D$ where $\mathbf{S}_P$ and $\mathbf{S}_D$ respectively contain the time-domain samples of the pilot blocks and data blocks with

$$(\mathbf{S}_P)_{i,j} = \begin{cases} s^p(i-j) & i=0,\ldots,N_TB_p-1, \\ & j=0,\ldots,L-1,\ i\geq j \\ 0 & i=N_TB_p,\ldots,N_T(B_p+B_s)-1, \\ & j=0,\ldots,L-1 \end{cases} \tag{7}$$

$$(\mathbf{S}_D)_{i,j} = \begin{cases} 0 & i=0,\ldots,N_TB_p-1 \\ & j=0,\ldots,L-1 \\ s^d(i-j) & i=N_TB_p,\ldots,N_T(B_p+B_s)-1, \\ & j=0,\ldots,L-1 \end{cases} \tag{8}$$

where $s^p(i-j)$ and $s^d(i-j)$ are the transmitted pilot and data time domain MC-CDMA samples respectively. Taking into account (7) and (8), we can break up $\mathbf{S}_\Delta = \mathbf{S}_{\Delta,P}+\mathbf{S}_{\Delta,D}$.

A. Initial ML Estimation

For the initial estimation, we consider only the pilot symbols, i.e. the unknown coded symbols are ignored. In that case, the observation model yields $\mathbf{r} = \mathbf{S}_{\Delta,P}\mathbf{h}+\mathbf{w}+\mathbf{Int}$. The initial ML estimate of the delay and channel taps is obtained as [1]:

$$\left[\hat{\Delta},\hat{\mathbf{h}}\right] = \arg\max_{\Delta,\mathbf{h}}\{\mathbf{log}\ p(\mathbf{r}\,|\mathbf{S}_{\Delta,P},\mathbf{h})\} \tag{9}$$

where

$$log\ p(\mathbf{r}\,|\mathbf{S}_{\Delta,P},\mathbf{h}) \propto \left\{-(\mathbf{r}-\mathbf{S}_{\Delta,P}\mathbf{h})^H\mathbf{C}_x^{-1}(\mathbf{r}-\mathbf{S}_{\Delta,P}\mathbf{h})\right\} \tag{10}$$

and $\mathbf{C_x}$ is the covariance matrix given by

$$\begin{aligned}[\mathbf{C_x}]_{k,k'} &= E\left[(\mathbf{w}(k)+\mathbf{I}(k))(\mathbf{w}(k')+\mathbf{I}(k'))^H\right] \\ &= 2\sigma^2 + \\ &\quad \sum_{l=1}^{N_I}E_l\sum_{h=-\infty}^{\infty}g_l(kT_0-hT_l)g_l^*(k'T_0-hT_l)\end{aligned} \tag{11}$$

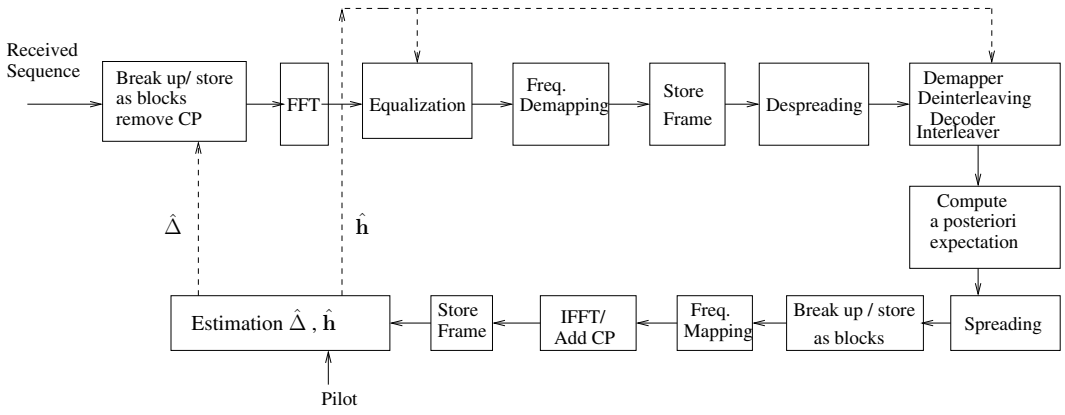

Fig. 2. The conceptual block diagram of the receiver

We assume that the delay Δ belongs to the range $\{0, 1, \ldots \Delta_{max}\}$. For each value of Δ, the corresponding estimated channel $\hat{\mathbf{h}}_{\boldsymbol{\Delta}}$ can be found in closed form as

$$\hat{\mathbf{h}}_{\Delta} = \left(\mathbf{S}_{\Delta,P}^{H}\mathbf{C}_{x}^{-1}\mathbf{S}_{\Delta,P}\right)^{-1}\mathbf{S}_{\Delta,P}^{H}\mathbf{C}_{x}^{-1}\mathbf{r} \tag{12}$$

Further, we use (12) to perform a one-dimensional search to find value for Δ:

$$\hat{\Delta} = \arg\max_{\Delta}\left\{\log p\left(\mathbf{r}\left|\mathbf{S}_{\Delta,P}, \hat{\mathbf{h}}_{\Delta}\right.\right)\right\} \tag{13}$$

Finally, the channel estimate yields $\hat{\mathbf{h}} = \hat{\mathbf{h}}_{\hat{\Delta}}$.

B. Soft Information Aided Estimation

The estimates of the previous section can be used as initial estimates in an iterative soft information aided estimation. We now use as observation model not only the pilot symbols as in the previous section, but we also take into account the data symbols. We follow the same reasoning as in [1] and take into account the statistical properties of the NBI through $\mathbf{C}_{\mathbf{x}}$. The updates of the delay and the channel taps at iteration ξ can then be written as :

$$\hat{\mathbf{h}}_{\Delta}(\xi+1) = \left(\widetilde{\mathbf{S}}_{\Delta(\xi)}^{H}\mathbf{C}_{x}^{-1}\widetilde{\mathbf{S}}_{\Delta(\xi)}\right)^{-1}\widetilde{\mathbf{S}}_{\Delta(\xi)}^{H}\mathbf{C}_{x}^{-1}\mathbf{r} \tag{14}$$

$$\hat{\Delta}(\xi+1) = \arg\max_{\Delta}\left\{-\left(\mathbf{r}-\widetilde{\mathbf{X}}_{\boldsymbol{\Delta}(\xi)}\right)^{H}\mathbf{C}_{x}^{-1}\left(\mathbf{r}-\widetilde{\mathbf{X}}_{\boldsymbol{\Delta}(\xi)}\right)\right\} \tag{15}$$

where $\widetilde{\mathbf{X}}_{\boldsymbol{\Delta}(\xi)} = \widetilde{\mathbf{S}}_{\boldsymbol{\Delta}(\xi)}\mathbf{h}_{\boldsymbol{\Delta}(\xi)}$, $\widetilde{\mathbf{S}}_{\Delta(\xi)}$ is obtained by replacing in (1) $s_{j,n}^{(k')}$ with their corresponding a posteriori expectations $E\left[s_{i,m}^{(k')}\middle|\mathbf{r}, \hat{\theta}(\xi)\right]$, where $\hat{\theta}(\xi) = \left[\hat{\Delta}(\xi)\ \hat{\mathbf{h}}(\xi)\right]$. Finally, the estimated channel $\hat{\mathbf{h}}(\xi+1) = \hat{\mathbf{h}}_{\hat{\Delta}}(\xi+1)$.

IV. Numerical Results

To validate the proposed algorithm, we have carried out Monte Carlo simulations. We consider a system with $M = 1$ user, using a convolutional code with constraint length 5, rate $R = 1/2$ and polynomial generators $(23)_8$ and $(35)_8$. A block length of $X_b = 240$ information bits was chosen, leading to $X_c = 480$ coded bits. Coded bits are Gray-mapped onto an 8-PSK constellation, resulting in $X_d = 160$ data symbols. This sequence of N_d 8-PSK symbols is broken up into $B_s = 20$ blocks of $Q = 8$ symbols. Spreading sequences are real-valued Walsh-Hadamard sequences, with chips belonging to $\left\{-\frac{1}{\sqrt{N_s}}, +\frac{1}{\sqrt{N_s}}\right\}$ and have a length $N_s = 32$, leading to $N = QN_s = 256$ required subcarriers. To initialize the EM algorithm, the B_s data MC symbols are preceded by $B_p = 1$ pilot MC symbol. Within the pilot MC symbol, only 25% of the subcarriers are devoted to training. The remaining 75% of the carriers is reserved for administrative data, and cannot be used during the synchronization/estimation process. The channel has length $L = 15$ and was modeled with independent components, each component being a zero-mean complex Gaussian random variable with an exponential power delay profile [1]:

$$E\left[\left|h(l)\right|^2\right] = E_h \exp(-l/5),\ l = 0, \ldots, L-1 \tag{16}$$

where E_h is chosen such that the average energy per subcarrier is normalized to unity. Hence, the energy of the channel is concentrated mainly in the first few channel taps. To avoid ISI, a cyclic prefix of length $\nu = 16$ is employed. Further, transmit filters are square-root raised-cosine filters with roll off factors $\alpha_0 = 0.25$ and $\alpha_l = 0.5$ for MC and interfering signals, respectively. We assume $N_I = 1$ interferer and $f_{c,1} = 0$. The bandwidths of the MC and interferer spectrum equal $B_0 = \frac{1}{T_0} = 1024$ kHz and $B_1 = \frac{1}{T_1} = 25$ kHz. We use QPSK modulation for the interferer signals. The time delay of the interferer equals $\tau_1 = 0$.

Figure 3 shows the mean squared estimation error σ_h^2 of the channel for both the original and the modified algorithm, assuming perfect timing synchronization ($\Delta = 0$), as a function of the signal to interference ratio (SIR). As can be observed, a strong improvement of σ_h^2 is achieved after two iterations. At low values of SIR, σ_h^2 decreases for increasing SIR. At high values of SIR, σ_h^2 is independent of the SIR as the effect of the NBI diminishes. As expected, the modified algorithm performs better than the original algorithm at low

values of SIR. However, at high values of SIR, σ_h^2 for both algorithms converge to the same asymptote, corresponding to the case where no interference is present. This asymptote is determined by the signal to noise ratio (E_b/N_0).

Figure 4 shows the probability of false synchronization P_f assuming perfect channel estimation for both algorithms as function of SIR. As can be observed, a large improvement is achieved after the first iteration. At low values of SIR, the modified algorithm is better than the original algorithm. However, at high values of SIR, P_f of both algorithms reach the same asymptote, corresponding to the case where no interference is present.

Figure 5 shows the BER performance, assuming perfect timing synchronization ($\Delta = 0$). As can be observed, when performing data-aided channel estimation, the BER degradation as compared to perfect channel knowledge is unacceptable. Soft information aided estimation is able to reduce this degradation to around 1 dB after 2 iterations. The BER of the modified algorithm shows an improvement as compared to the original algorithm.

Figure 6 show BER performance for the delay estimator, assuming perfect channel estimation. The BER performance of the modified algorithm shows an improvement as compared to the original algorithm.

Figure 7 shows the BER performance for joint frame synchronization and channel estimation for the two algorithms. As expected, the data aided estimator (iteration 0) gives rise to large degradations. On the other hand, soft information aided algorithm has good performance after two iterations.

V. Conclusions

We adapt the code aided joint frame synchronization and channel estimation algorithm for downlink MC-CDMA presented in [1] to have better performance in the presence of narrowband interference. The performance of the modified algorithm is compared to the original algorithm in the following three scenarios: first, we consider the estimation of the channel impulse response, assuming perfect timing synchronization. Next, we consider the estimation of the frame delay, assuming perfect channel estimation. Finally, we consider joint channel estimation and frame synchronization. The results indicate that the modified algorithm has better MSEE performance and lower probability of false synchronization than the original algorithm. Further, BER of the modified algorithm slightly outperforms the one of the original algorithm.

References

[1] M. Guenach, H. Wymeersch, H. Steendam and M. Moeneclaey. "Code-aided ML Joint Synchronization and Channel Estimation for Downlink MC-CDMA ". *IEEE Journal on Selected Areas in Comm.*, vol. 24(6):pp. 1105–1114, Jun. 2006.

[2] J.A.C. Bingham. "Multicarrier Modulation for Data Transmission: An Idea Whose Time Has Come". *IEEE Comm. Mag.*, vol. 28(5):pp.5–14, 1990.

[3] T. Keller and L. Hanzo. "Adaptive Multicarrier Modulation: A Convenient Framework for Time-Frequency Processing in Wireless Communications ". *IEEE Proceedings of The IEEE.*, vol. 88:pp. 611–640, May. 2000.

[4] M. Marey and H. Steendam. "The Effect of Narrowband Interference on the Timing Synchronization for OFDM Systems". In *Proc. of the 12th IEEE Benelux Symposium on Communications and Vehicular Technology*, Nov. 2005.

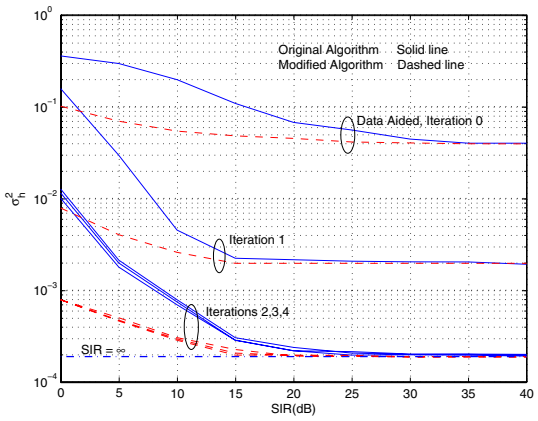

Fig. 3. MSEE performance, perfect synchronization is assumed E_b/N_o= 12 dB.

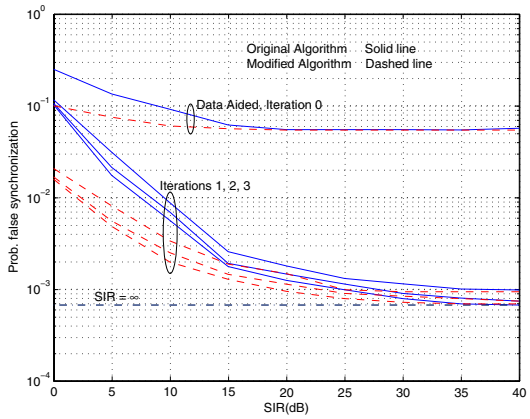

Fig. 4. Probability of false synchronization, perfect channel estimation is assumed, E_b/N_o= 12 dB

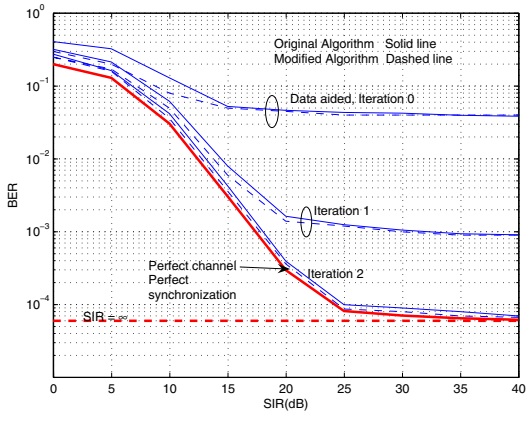

Fig. 5. BER performance, perfect synchronization is assumed E_b/N_o= 12 dB

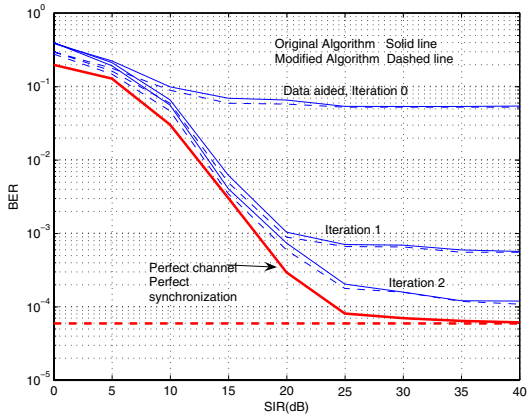

Fig. 6. BER performance, perfect channel estimation is assumed, E_b/N_o= 12 dB

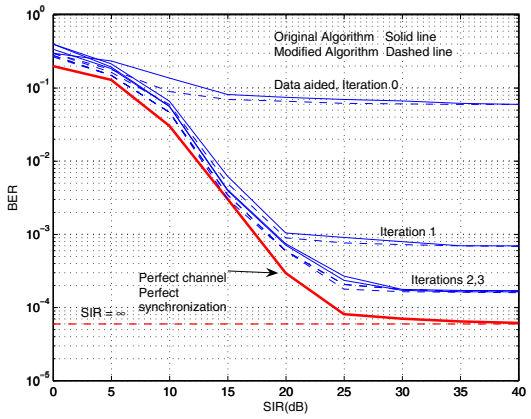

Fig. 7. BER performance, E_b/N_o= 12 dB

[5] M. Marey and H. Steendam. "The Effect of Narrowband Interference on Frequency Ambiguity Resolution for OFDM". In *Proc. of Vehicular Technology Conference Fall 2006*, Montréal, Canada, Sept. 2006.

[6] M. Marey and H. Steendam. "The Effect of Narrowband Interference on ML Fractional Frequency Offset Estimator for OFDM". In *Proc. of International Mobile Multimedia Communications*, Alghero, Italy, Sept. 2006.

[7] `http://www.b-vhf.org`.

[8] D. Zhang, P. Fan, and Z. Cao . "Interference Cancellation for OFDM Systems in Presence of Overlapped Narrow Band Transmission System". *IEEE Trans. on Consumer Electronics.*, vol. 50(1):pp. 108–114, Feb. 2004.